Turk. J. Fish.& Aquat. Sci. 24(8), TRJFAS24612
https://doi.org/10.4194/TRJFAS24612

PROOF
RESEARCH PAPER

Turkish Journal of FISHERIES and AQUATIC SCIENCES

Seasonal and Inter-annual Variability in the East of the Sea of Marmara Water Masses by Temperature and Salinity Time Series

Kubilay Dökümcü[1, 2*], Hüsne Altıok[1]

[1]Istanbul University Institute of Marine Sciences and Management, Istanbul/Türkiye)
[2]Istanbul Technical University, Department of Shipbuilding and Ocean Engineering, Istanbul, Türkiye.

How to Cite

Dökümcü, K., Altıok, H. (2024). Seasonal and Inter-annual Variability in the East of the Sea of Marmara Water Masses by Temperature and Salinity Time Series. *Turkish Journal of Fisheries and Aquatic Sciences*, *24(8), TRJFAS24612.* https://doi.org/10.4194/TRJFAS24612

Article History
Received 30 August 2023
Accepted 01 June 2024
First Online 12 June 2024

Corresponding Author
E-mail: kubilaydokumcu@gmail.com

Keywords
Climate change
Trend analysis
Temperature
Salinity
Sea of Marmara

Abstract

This study mainly aims to examine the relationship between oceanographic properties and climate change in the conjunction of the Istanbul Strait (IS), specifically in the east of the Sea of Marmara (SoM) via evaluating observational temperature and salinity profiles at six stations with monthly atmospheric pressure and air temperature during the period of 1997-2010. The annual cycle of temperature and salinity of the upper and lower layers in the east of SoM have strong seasonal variation: The upper layer temperature rises during summer while decreases in winter. Conversely, the lower layer temperature is higher in winter compared to spring and summer. Additionally, salinity levels in the upper layer are higher in winter and lower in summer, whereas in the lower layer, the pattern is reversed, with lower salinity in winter and higher salinity in summer. In this context, linear trend analyzes are calculated by using monthly time series of temperature and salinity and compared with the trends of atmospheric conditions and the surrounding seas. The average temperature trend in the east of the SoM is increase of 0.067°C/y in the upper layer and increase of 0.028°C/y in the lower layer during this period. The salinity trend is increase of 0.105 psu/y in the upper layer and increase of 0.012 psu/y in the lower layer. The air temperature trend is increase of 0.086°C/y, and the air pressure trend is decrease of 0.034 mbar/y. These values closely align with those observed in the surrounding seas. The air temperature and upper layer temperatures are consistent with each other in terms of both long-term series and trend values.

Introduction

The increase in sea surface temperature (SST) in the oceans is a crucial indicator of the climate change. The effect of ocean warming causes to change the ecosystem structure as whitening coral reef, jellyfish bloom, food-web (Edwards, 2016). It has been also observed that extreme natural events such as mucilage have occurred with increasing frequency in the Adriatic Sea and Sea of Marmara (SoM) since the 1950s with global warming (Danovaro et al., 2009). Temperature increase due to climatic conditions are generally higher in enclosed than in open systems (Philippart et al., 2011). SoM, as a semi-enclosed sea, is expected influenced by global warming with increase of SST.

SoM has a unique ecosystem as a part of Turkish Straits System with its interaction between Mediterranean Sea (MS) and Black Sea (BS) which have very different oceanographic properties. In BS, the average sea surface temperature stands at approximately 8°C during winter months and rises to around 23-24°C during summer. In MS, temperature exhibit a range typically between 15-18°C. Sea surface salinity in BS varies around 18-19‰, showing a slight decrease at depths of 20-30 meters before stabilizing around 22.4‰ from 200 meters depth onwards. In

contrast, salinity in MS remains relatively constant around 38-39‰ regardless of depth (Schroeder et al., 2023; Özsoy and Ünlüata, 1997). It is a semi-enclosed basin with the area of 11500 km^2 which connects the BS through Istanbul Strait (IS) and MS through the Canakkale Strait (Figure 1).

A sharp density interface is observed at a depth of 25 m, where the upper layer originated from brackish waters with a salinity of 18 psu, and the lower layer originated from highly saline waters with a salinity of 38.5 psu. The upper and lower layers exhibit renewal times of 3-4 months and 6-7 years, respectively. The upper layer is subject to turbulent entrainment into the exit region of the IS jet, as well as wind-stirring in winter. Both processes contribute equally to the vertical mixing of the SoM. The upper layer salinity is within the range of 23±2 ppt, reaching a maximum in winter as a consequence of increased wind mixing in the basin and a reduction in the influx from the Black Sea. During the winter, the eruption of the halocline can broaden it, in contrast to its usual sharp interface at other times (Unluata et al., 1990; Besiktepe et al., 1994). The SoM has three deep basins (deeper than 1000m) oriented in the east-west direction. The study area encompasses the Cinarcik Basin, which is situated at the easternmost extent of the basins and marks the exit region of the IS (Figure 1). Consequently, the area is subject to the influence of the IS jet and wind-induced mixing.

So far, the impact of climate change on oceanographic parameters has been studied in the BS, MS, Aegean Sea (AS) and IS (D'Ortenzio et al., 2000; Lelieveld et al., 2002; Ginzburg et al., 2004; Theocharis, 2008; Vargas-Yanez et al., 2008; Belkin, 2009; Nykjaer, 2009; Skliris et al., 2011; Skliris et al., 2012; Shaltout & Omstedt, 2014; Altiok & Kayisoglu, 2015). However the lack of such a specific study in the SoM made it necessary to take a closer look and understand how climate change might affect the characteristics of the SoM.

Sea surface temperature (SST) of the SoM have been increasing for several decades as similar in neighboring seas BS and MS. The trend analysis based on different methods and different time scale indicated that increasing of the BS SST is the range of 0.05-0.09°C/y since 1980's (Ginzburg et al., 2004; Belkin, 2009; Shaltout & Omstedt, 2014). The general observation of a value for AS SST trend is around ~0.05°C/y (Theocharis, 2008; Skliris et al., 2011; Shaltout & Omstedt, 2014, Tukenmez & Altiok, 2022), Serykh and Kostianoy (2021) have identified a trend of 0.01°C/y between 1955 and 2015. Besides, MS SST trend takes constant values between 0.03 and 0.04°C/y (D'Ortenzio et al., 2000; Lelieveld et al., 2002; Vargas-Yanez et al., 2008; Nykjaer, 2009; Skliris et al., 2012). Altiok and Kayisoglu (2015) analyzed the upper layer temperature data of the IS, which connects the SoM with the BS, and obtained values of 0.07°C/y at the northern exit, and 0.15°C/y at the southern exit between 1996 and 2010. Furthermore, there is a diminish in the Cold Intermediate Layer (CIL), which is very important for the BS suboxic zone because of its high oxygen content. It is not only important for elucidating the water mass dynamics but can also contribute to understanding the dynamics of the ecosystem. Changes in the thermohaline structure seem to play a crucial role in the exchange of nutrients and biological matter, potentially altering food-web dynamics across various time scales. The formation mechanisms CIL have weakened in the last 10 years, leading to both an increase in temperature and a decrease in its thickness (Miladivona et al., 2018, Gunduz et al., 2020). The warming trend of the CIL is calculated ~0.05°C/y and this trend is higher in the last 10 years (Stanev et al., 2019). According to another comprehensive study, the core temperature of CIL was increased about 2.0°C over the past 25 years (von Schuckmann et al., 2020).

In the northern entrance of the IS the temperature of the upper layer coming from the BS has increasing trend of 0.07°C/y between 1996-2010 based on monthly measured data (Altiok & Kayisoglu, 2015). Although the time series is not long enough to conclude the long term trend it can be said that this value is similar that of BS SST warming trend (0.05-0.09°C/y since 1980's, Ginzburg et al., 2004; Belkin, 2009; Shaltout and Omstedt, 2014). On the other hand, in the southern exit of IS, the upper layer temperature trend of 0.15°C/y is very high during the same period. Altiok and Kayisoglu (2015) claim that this increase may have been caused variability of the CIL along the strait and a mixing the layers. Similar as upper layer the trends of 0.06-0.07°C/y were found in the lower layer temperature in both exit of the strait which is higher than AS and MS (0.04-0.05°C/y for AS and 0.03-0.04°C/y for MS, Skliris et al. 2011; Shaltout & Omstedt 2014). The salinity of the lower layer has also positive trend at both exits while there is not any change in the upper layer salinity during the same period (Altiok & Kayisoglu, 2015).

The aim of this study is to investigate the seasonal and interannual variability of the water masses temperature and salinity in the east of the SoM. For this purpose, monthly time series of temperature and salinity of the layers as well as air pressure and temperature are presented. CTD (Conductivity-Temperature-Depth) data covers the 13-year data set (1997- 2010) and, meteorological data covers the 22-year data set (1997-2019). In order to determine the climate change trend analysis was performed for the parameters.

Materials and Methods

The region defined as east of the SoM is the region between longitudes 28 °36' E and 29 °20' E and latitudes 40 °42' N and 40 °59' N as shown in Figure 2. The location information of the stations where measurements were made is as in Table 1. CTD measurements at stations 45C and MY2 were carried out in April and October in 2019.

Figure 1. BS, MS and AS (Study area can be seen in red rectangular. Changed from https://visibleearth.nasa.gov/images/66903/sea-of-marmara-turkey).

The CTD data used in this study were collected from the stations in the east of the SoM (Figure 2, Table 1) on board the R/V ARAR operated by Istanbul University, Institute of Marine Sciences and Management (IMSM-IU). Monthly measurements were consistently performed on the designated day, but occasional delays of 1-2 days occurred due to severe weather conditions. CTD data were collected between 1997-2010 using the Seabird SBE911 system and the Seabird SBE25 Sealogger. The measurement accuracy of the conductivity sensor is 0.001 S/m, and the sensitivity is 0.00004 S/m, while the measurement accuracy of the temperature sensor is 0.01°C and the sensitivity is 0.0003 °C. The data collected by the two instruments at the same time and location were analyzed and compared. The differences were 0.03°C between temperature profiles and 0.014 psu between salinity profiles. Temperature and salinity data quality were checked manually after cruise and the bad data were eliminated.

To elucidate the interdependencies of atmospheric and oceanographic variables, we employed monthly air temperature and atmospheric pressure data spanning from 1997 to 2019, collected by the Florya Meteorological Station of the Turkish State Meteorological Service (TSMS).

Mean values were calculated for each monthly dataset to elucidate the inherent seasonal variations within air temperature, air pressure, upper and lower layer temperature and salinity profiles. Since two layer stratification in SoM is under the influence of the baroclinic and barotrophic forcing caused by mainly atmospheric forcing the thickness of the layers are very changable. Instead of employing average salinity and temperature values for the upper and lower layers, values representing specific depths were utilized. For the upper layer time series, temperature and salinity at 5 m depth were chosen as good indicators to monitor the seasonal variations in the upper layer waters coming from the Black Sea. The 40-meter depth was chosen because it provides data beneath the pycnocline and offers more precise information. Additionally, it represents conditions in the Mediterranean Sea. It is noteworthy that data at both 5 and 40 meters are available at all stations, which further informed our selection criteria. Additionally, a linear trend analysis was conducted separately for the upper and lower layers of the water column:

$$y = a + bx$$

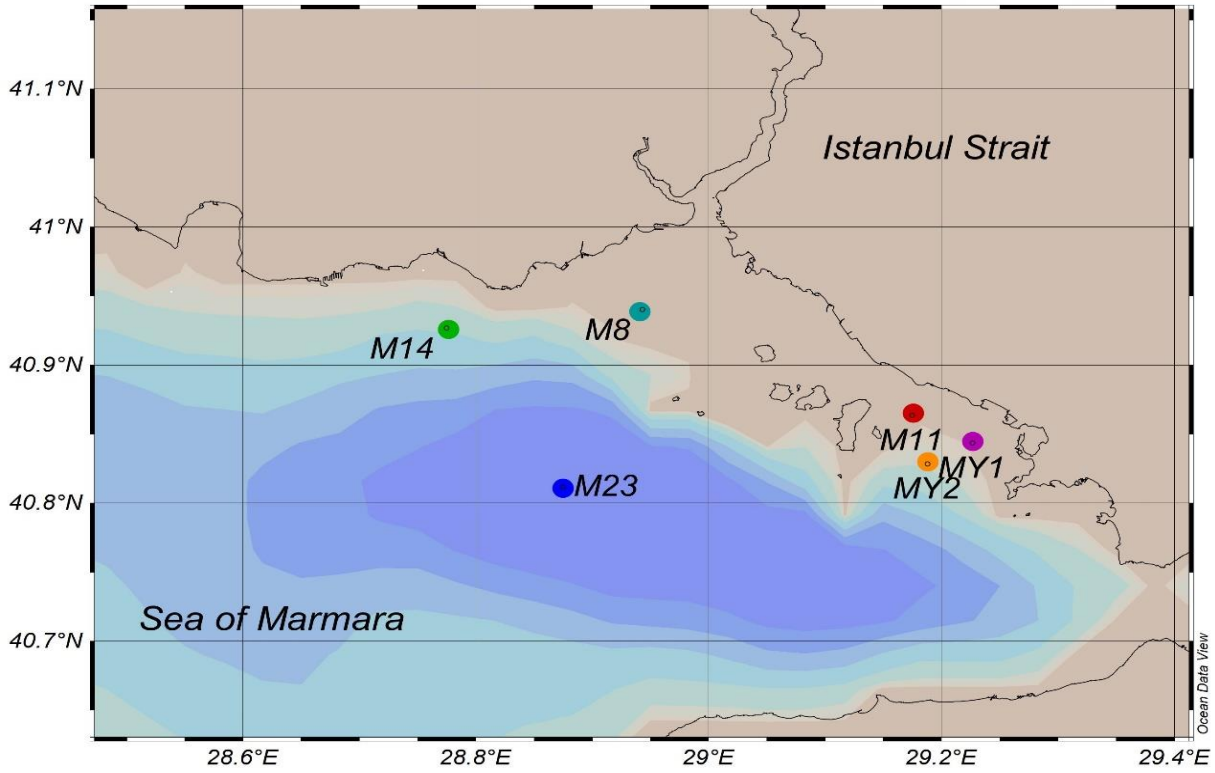

Figure 2. Locations of stations.

Table 1. Coordinates of the stations and measurement period and frequency/missing data (Obs.Freq.: Observation frequencies).

Station	Lat. (N)	Long. (E)	Depth (m)	Period	Obs. Freq.	Missing Data
M8	40.94	28.94	65	February 1997-January 2010	0.94	January 1999, February 1999, March 1997, March 2009, April 1997, April 2008, July 2007, September 2008, October 1997, October 1998
M23	40.81	28.88	1240	February 1997-January 2010	0.87	January 1999, January 2000, January 2006, February 1999, February 2001, February 2004, March 1997, March 2009, April 1997, April 2008, May 2005, June 2003, July 2007, September 2001, September 2004, September 2006, September 2008, October 1997, October 1998, December 1998, December 2007
M11	40.86	29.18	63	February 1997-January 2010	0.9	January 1999, February 1999, February 2009, March 1997, March 2009, April 1997, April 2008, June 1999, July 1999, August 2007, September 2008, October 1997, October 1998, October 1999, December 1999
MY1	40.84	29.23	42	June 1997-January 2010	0.91	January 1999, January 2006, January 2009, February 1999, February 2009, March 2009, April 2001, April 2008, May 2005, June 2003, July 2007, September 2008, October 1997, October 1998
MY2	40.83	29.19	91	March 1999-January 2010, May 2019 and October 2019	0.9	January 2006, January 2009, February 2009, March 2009, April 2001, April 2008, May 2005, May 2009, June 2003, July 2007, August 2006, September 2008, October 2000
M14	40.93	28.78	85	February 1997-January 2010	0.88	January 1999, January 2006, February 1999, February 2009, March 1997, March 2009, April 1997, April 2005, April 2008, May 2005, May 2009, June 2003, July 2007, August 2007, September 2008, October 1997, October 1998, October 1999, December 1999
45C	40.79	28.89	1300	May 2019, October 2019	-	-

Linear trend refers to a pattern or tendency where the dependent variable (usually denoted as “y”) changes in a linear manner over time (represented by the independent variable, denoted as “x”). In other words, the relationship between the two variables can be described by a straight line. To determine the linear trend, data is collected from past periods and analyzed using the equation as seen above. In this equation, “a” represents the constant coefficient or the intercept of the line, and “b” represents the slope or the trend of the line. The value of “x” represents time, which is used to estimate the value of “y” at different points in time.

The CIL thickness was calculated in accordance with the methodology proposed by Altıok et al. (2012), which considers a temperature of 14°C or below as the threshold for calculating the thickness for each year when the surface temperature is greater than 14°C. This average is then applied to every station.

In addition to the linear trend, the moving average method was used to determine the trends of atmospheric data. Moving average is a time-based, lagged indicator that shows the average of a parameter (temperature or pressure) over a period of time. By using moving averages, it is aimed to smooth out the “noise” effect of meteorological data.

Results and Discussions

Variation of Atmospheric Parameters

Meteorological values representing the east of the SoM spanning between 1997 and 2019 are analyzed and presented in Figure 3. It is observed that the air temperature is generally low in January and February and high in July and August. According to the mean temperature values, the coldest month is February 2003. February 2003 mean temperature values showed an anomaly from both other February records and other months. While the mean February temperature values across other years oscillated between 5.3 to 8.2°C, the mean temperature for February 2003 was notably lower at 2.2°C. This resulted in the lowest upper layer water temperature at the majority of monitoring stations on this particular date. Likewise, the month of January 2000 exhibited cold conditions, characterized by a mean temperature of 3.4°C, with a daily minimum reaching as low as -7.0°C. Subsequent to the year 2010, the lowest average temperature manifested in the month of January 2017, registering at 3.5°C, accompanied by a daily minimum of -6.3°C.

The maximum thermal anomaly was recorded in the month of August 2010, exhibiting an average temperature of 27.4°C. Following closely, July 2001 and July 2002 emerge as the subsequent two warmest months, recording temperatures of 26.9°C and 26.6°C, respectively. Notable peaks also include 38.5°C in August 2002 and 37.4°C in July 2000, denoting an intense heatwave during the summer interval spanning from 2000 to 2002. It is crucial to highlight an intriguing datum: an occurrence of average temperatures equal to or surpassing 25°C was observed for 13 months within the 13-year interval between January 1997 and December 2009, whereas this trend expanded to encompass 15 months during a decade from January 2010 to December 2019. In sum, the prevalence of temperatures exceeding the 25°C threshold escalated from 8% in the late 1990s and 2000s to 13% in the 2010s.

Anticyclones, areas of intense high pressure typically above 1020 mb, are a common feature of midlatitude climate and are associated with descending air conditions, and associated anticyclonic circulation anomalies can contribute to temperature anomalies (Pepler, 2023). Based on the analysis of monthly atmospheric pressure data, it is evident that the three months displaying the highest mean values are December 2015, recording an average of 1025 mbar, December 2006 with 1022.2 mbar, and February 2008 at 1022 mbar. During these months, anticyclonic air currents prevailed, resulting in notably cold and foggy conditions. Within the period of 1997-2019, the atmospheric pressure exceeded the average threshold of 1020 mbar on 8 occasions. Among these, 4 instances occurred prior to 2010, while the remaining 4 took place during the 2010s. The consistent frequency of months surpassing the 1020 mbar threshold, both pre-2010 and post-2010, implies a stable occurrence of anticyclonic patterns throughout the studied timeframe.

The three highest daily pressure values were recorded in December 2016 (1036 mbar), January 2015 (1034 mbar), and January 2008 (1034.7 mbar). These findings underscore the high pressure levels during winter months, particularly in the period of December to January. Conversely, the three months exhibiting the lowest average monthly pressure values were July 2018 (1004.8 mbar), August 2006 (1004.9 mbar), and June 2018 (1005.6 mbar), exhibiting a decline during the summer months. Notably, the year 2008 presents an anomaly in terms of air pressure values, wherein a contrast between the low pressure in March 2008 immediately following the high pressure in February 2008 is observed. Additionally, the record for the lowest daily pressure reading occurred in November 2008, registering an exceptional value of 980.8 psu.

When examining the trends in atmospheric conditions, it becomes evident that there has been an annual increase of 0.085°C in the mean air temperature values. This increase corresponds to the more frequent occurrence of monthly mean temperatures exceeding 25°C during the 2010s. The analysis also revealed a reduction of 0.034 mbar in the mean annual air pressure values, a finding deemed negligible in significance (The derived linear fit formulas are as follows: For air temperature (Y) as a function of time (in years), the equation is Y=0.085 * Time(year) - 156.13. For air pressure (Y) as a function of time (in years), the equation is Y=-0.034 * Time(year) + 1080.94.).

The temperature trend graph prepared in order to determine the trend of air temperature between 1997-2008 and 2009-2019 separately and to compare the temperature trends in the first and second half of the period analyzed is presented in Figure 4a, 4b. The temperature trend between 1997 and 2008 registers at increase of 0.06°C/y. Conversely, the period between 2009 and 2019 exhibits an increasing temperature trend of 0.11°C/y, nearly doubling the trend observed in the former half. The reason for the nearly doubled trend compared to the first half is considered to be related to the fact that nine of the ten warmest years since 1880 globally occurred after 2005 (Lindsey & Dahlman, 2020).

Seasonal and Annual Variations in Sea Temperature and Salinity

Upper Layer

In the seasonal analysis depicted in Figure 5a, 5b and Table 2, examination of station means reveals distinct sea temperature and salinity patterns within the upper layer. Summer months exhibit warmer sea temperature and lower salinity, while winter months display cooler temperature and higher salinity, as expected. The upper layer experiences lower salinity during spring and summer due to high freshwater influx from the BS. Notably, at station M8, situated at the IS

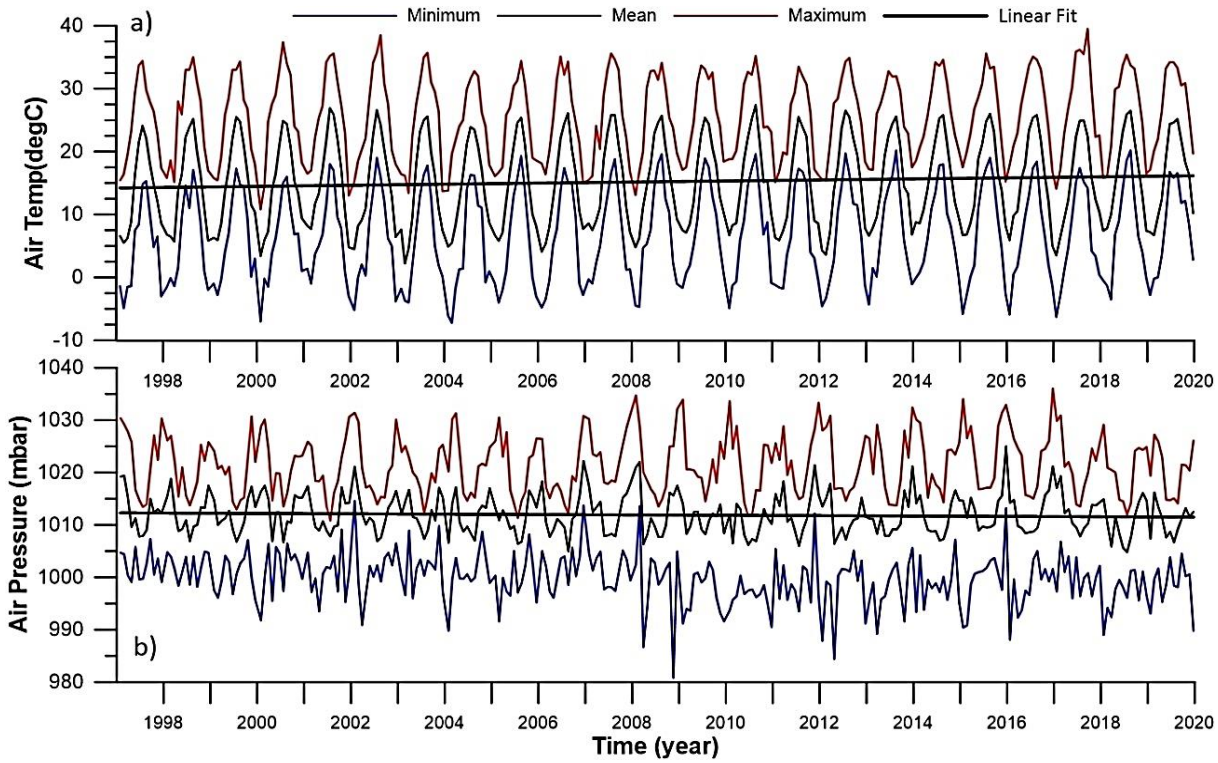

Figure 3. Monthly and long-term changes in air temperature (a) and pressure (b) at the Florya Meteorology Station (Analyzed from TSMS data).

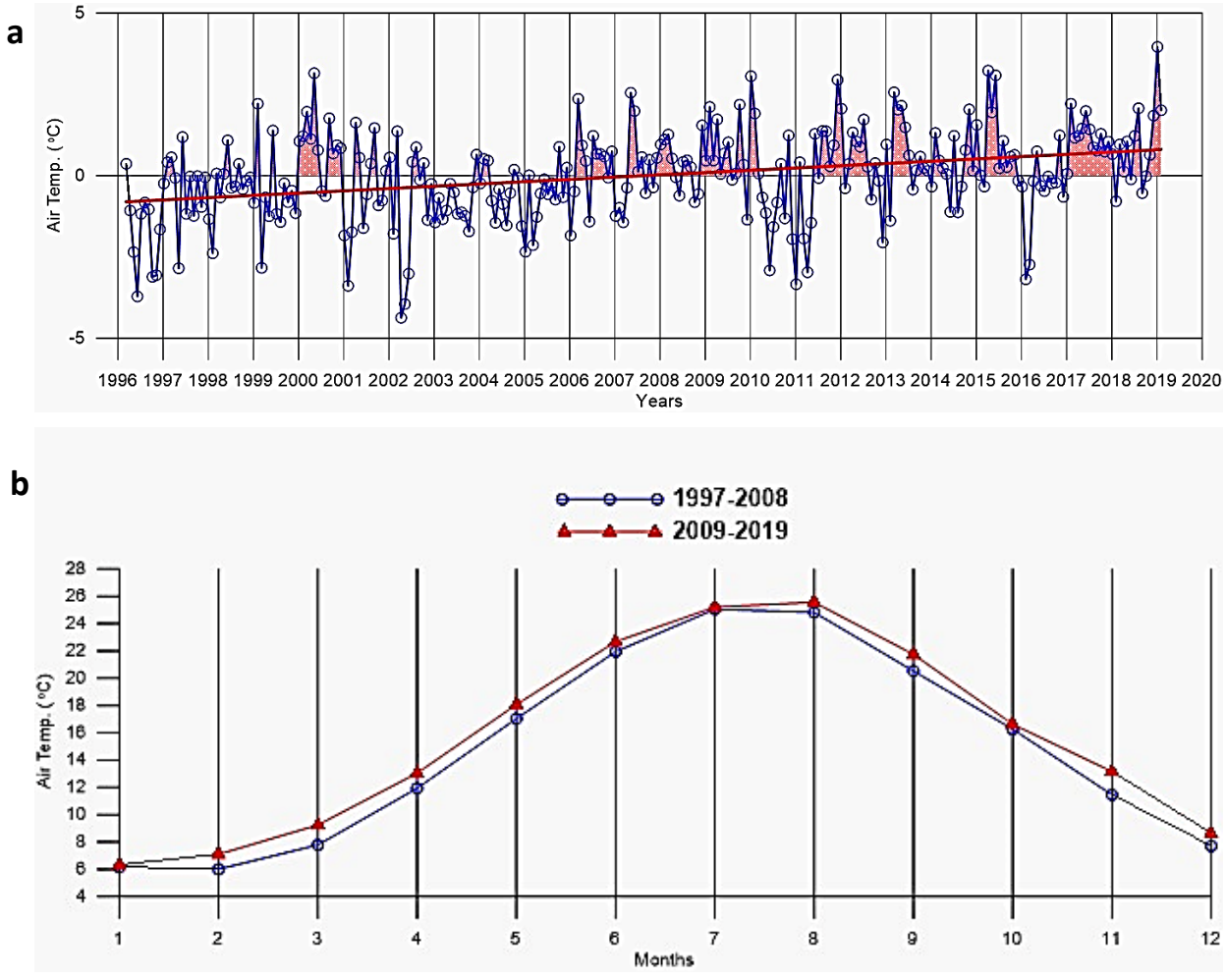

Figure 4. Air temperature annual (a), monthly (b) mean values.

exit, MS effects are evident exclusively in December, marked by salinity values exceeding 24 psu. Similarly, station M23, slightly farther out, exhibits this effect with values surpassing 25 psu in both January and December, as well as exceeding 24 psu in November, signifying an extended and intensified influence of MS. Transitioning east of IS, all three stations (M11, MY1, MY2) showcase salinity values surpassing 26 psu in January and December, and exceeding 25 psu in February and November, diverging from those at the IS exit. M14, station situated west of the IS, exhibit salinity characteristics akin to those observed at the IS exit.

CIL

A cold intermediate layer is observed in the MS during the summer months, situated just above the halocline. This layer is thought to be partially formed within the Sea of Marmara in the winter months and partially advected from the Black Sea (Ünlüata et al. 1990). Altıok et al., (2012) evaluated the salinity and temperature data collected monthly between 1996 and 2000 and determined that CIL occurs at depths where the temperature is colder than 14°C in IS and its southern exit to MS. At the northern exit of IS, CIL occurs between April-October and at the southern exit, it occurs between May-October. Proceeding southern from that point, the layer thickness decreases due to mixing.

In this study, the occurrence of CIL at depths where the temperature is colder than 14°C between May and August (M23 exceptional, September also) is consistent with the findings of Altıok et al. (2021). The CIL thicknesses formed according to the mean temperatures in the stations are presented in Figure 5e, and the lowest temperature in the layer thickness and the salinity values at the depth where this temperature is located are presented in Table 3.

While occasional observations were made in April and September at certain stations and years, a consistent prevalence of the CIL was ascertained during the May to August period, based on mean sea temperature profiles. This layer showed different thicknesses: 16-21 meters in May, 10-16 meters in June, 9-11 meters in July, and 5-8 meters in August. The similar values among stations indicated consistency in layer thickness. Notably, only station M23 had a 2-meter thick CIL in September, with temperatures close to 14°C (around 13.90°C and 13.96°C). The other exceptional instance occurred in April 2005 at MY2 station. However, the CIL was a consequence of the surface water exceeding 14°C in thickness by a few meters. The month of May is characterized by a comparatively greater thickness of CIL in comparison to the subsequent months. For the month of July, a significant finding was the 17-meter layer thickness at station M11. In the CIL, the lowest temperatures were recorded at 10.6-10.9°C in May, 11.4-11.7°C in June, 11.7-12.3°C in July, and 12.8-13.5°C in August. Salinity measurements at these lower temperature levels exhibited variations ranging from 27 to 33 practical salinity units, fresher in May, saltier in August.

Lower Layer

Upon examination of substrate values in Figure 5c, 5d and Table 4, a notably narrow temperature range of 14.9-15.6°C is observed. In the winter months, temperatures are higher than in spring and summer, which differs from the upper layer temperature pattern. The lower layer is more stable, indicated by lower standard deviation values compared to the upper layer. Analysis of the mean salinity reveals a consistent mean structure akin to temperature readings, accompanied by low standard deviation. While the mean salinity ranges between 37.8-38.5 psu, lower salinity is observed during spring, contrasting with other seasons. This observation potentially traces back to the interaction between lower layer water and the diminishing freshwater influx from the BS, resulting in the springtime reduction of salinity. It is noteworthy that the lower layer salinity of station M23 is high. A salient observation is the pronounced higher salinity within the lower layer of station M23. This phenomenon finds its rationale in the geographical disposition of station M23, situated farther to the south and offshore of IS, experiencing more influences from MS.

Trend Analysis

The data collected at 5 meters was utilized to represent the upper layer, and the data at 40 meters was employed to depict the lower layer. These values were then used for comparative analysis with both previous research findings and the current dataset.

Figure 6 and Table 5 illustrate the temperature trends of the upper and lower layers within the east of the SoM. The annual increasing average temperature trend for the upper layer is calculated to be 0.067°C. Evident peaks in sea surface temperatures are observed in August 1999, July 2002, July 2003, and August 2005. Notably, the M14 station located west of the IS exhibits consistently higher temperature means compared to other regions. The annual temperature trend is increase of 0.067°C for the upper layer in the east of the SoM aligns closely with the temperature trends of neighboring seas, as detailed in Table 6. Comparatively, the temperature trend in the SoM is greater than that of the AS, and the MS, while being comparable to the trend seen in the BS. Importantly, none of the surrounding seas exhibit an annual temperature trend exceeding 0.1°C.

The bottom layer exhibits an annual average temperature trend of 0.028 °C, displaying peaks in December 2002, December 2004, February 2005, December 2009, and January 2010, while experiencing troughs in March 2002, March 2003, April 2003, March 2004, February 2006, and March 2006. Strong northerly

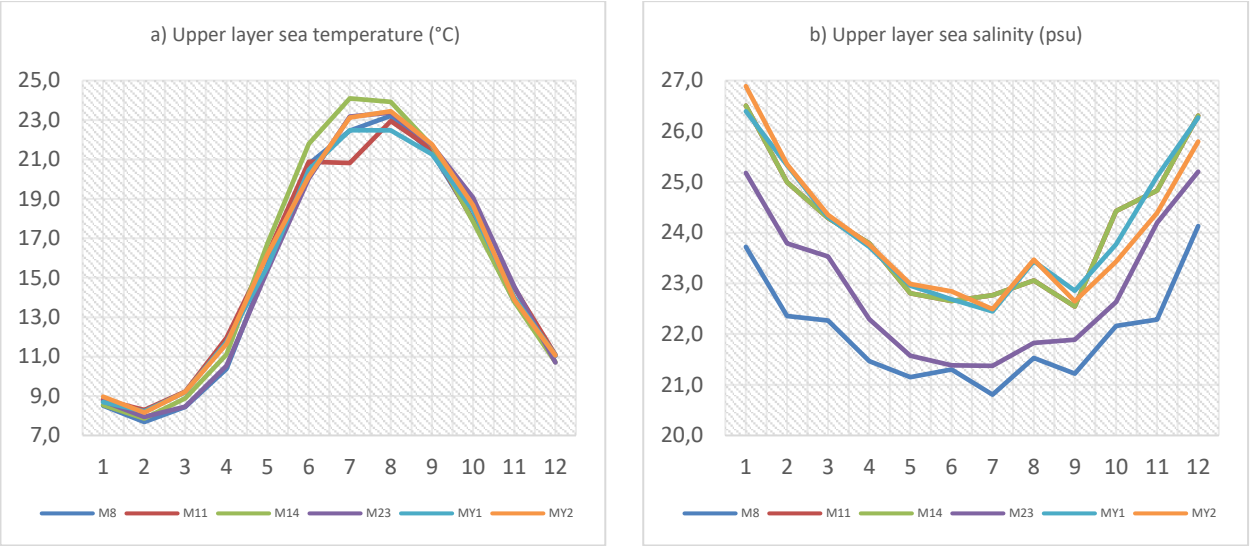

Figure 5. Upper layer (a, b) values (x-axis: Month).

Table 2. Upper layer mean sea temperature and salinity data (M: Month, std: Standard deviation, N: Count)

	M8					**M11**					**M14**				
M	T5	stdT	S5	stdS	N	T5	stdT	S5	stdS	N	T5	stdT	S5	stdS	N
1	8.5	1.2	23.7	1.6	11	8.8	1.2	26.5	2.1	10	8.7	0.9	26.4	2.5	10
2	7.7	1.2	22.4	1.1	12	8.3	0.7	25	1.3	10	8.2	0.8	25.3	1.4	10
3	8.5	1.4	22.3	1.2	11	9.2	1.4	24.3	1.1	11	9.2	1.4	24.3	1	11
4	10.4	1.7	21.5	1	11	12	1.7	23.8	1.3	10	11.7	1.7	23.7	1	10
5	15.6	2.1	21.1	0.8	13	16.2	1.7	22.8	1.1	11	15.6	2.1	23	1.3	11
6	20.8	2	21.3	0.7	13	20.9	2.2	22.7	0.9	12	20.5	2.1	22.7	0.6	12
7	22.5	2.9	20.8	0.9	12	20.8	2.1	22.8	0.8	12	22.5	1.6	22.4	0.8	12
8	23.2	1.5	21.5	1	13	22.9	1.1	23.1	1.3	13	22.5	1.2	23.4	1.2	13
9	21.4	0.9	21.2	0.5	12	21.5	1.2	22.5	1	12	21.3	1.2	22.9	1	12
10	18	1.3	22.2	1.7	11	17.9	1.2	24.4	1.7	11	18.4	1.3	23.8	1.2	11
11	13.8	1.3	22.3	1.8	13	14.5	1.8	24.8	2.1	13	14	1.6	25.1	2.1	13
12	11	1.5	24.1	2	13	11.1	1.4	26.3	2	13	11.1	1.4	26.3	2.1	13
	M23					**MY1**					**MY2**				
M	T5	stdT	S5	stdS	N	T5	stdT	S5	stdS	N	T5	stdT	S5	stdS	N
1	8.7	1	25.2	1.5	10	8.7	0.9	26.4	2.5	10	8.8	1.2	26.5	2.1	10
2	7.9	0.9	23.8	1.3	10	8.2	0.8	25.3	1.4	10	8.3	0.7	25	1.3	10
3	8.5	1	23.5	1.7	11	9.2	1.4	24.3	1	11	9.2	1.4	24.3	1.1	11
4	10.5	1.6	22.3	1.3	11	11.7	1.7	23.7	1	10	12	1.7	23.8	1.3	10
5	15.4	2.1	21.6	0.8	12	15.6	2.1	23	1.3	11	16.2	1.7	22.8	1.1	11
6	20	2.4	21.4	0.5	12	20.5	2.1	22.7	0.6	12	20.9	2.2	22.7	0.9	12
7	23.2	1.6	21.4	0.7	12	22.5	1.6	22.4	0.8	12	20.8	2.1	22.8	0.8	12
8	23.4	1.2	21.8	0.9	13	22.5	1.2	23.4	1.2	13	22.9	1.1	23.1	1.3	13
9	21.7	1.4	21.9	0.7	9	21.3	1.2	22.9	1	12	21.5	1.2	22.5	1	12
10	19.1	1.8	22.6	1.5	11	18.4	1.3	23.8	1.2	11	17.9	1.2	24.4	1.7	11
11	14.6	1.9	24.2	1.6	13	14	1.6	25.1	2.1	13	14.5	1.8	24.8	2.1	13
12	10.7	1.3	25.2	1.7	11	11.1	1.4	26.3	2.1	13	11.1	1.4	26.3	2	13

Table 3. CIL data (LT: Layer thickness (m), MT (°C), ST: Salinity at minimum temperature (psu)).

	May			**June**			**July**			**August**		
	LT	MT	ST	LT	MT	ST	LT	MT	ST	LT	MT	ST
M8	17	10.84	28.43	15	11.66	29	11	12.27	30.68	5	13.54	31.68
M11	20	10.65	27.25	16	11.41	28.91	17	11.68	27.65	7	13.04	30.95
M14	18	10.84	28.59	12	11.56	29.88	10	11.89	30.43	8	12.83	31.98
M23	16	10.64	28.84	10	11.68	30.55	9	11.78	29.77	6	13.1	32.57
MY1	20	10.85	28.3	14	11.58	29.17	11	12.04	29.83	7	13.21	31.02
MY2	21	10.92	29.53	15	11.68	28.95	10	12.23	29.98	6	13.45	32.99

Table 4. Lower layer mean sea temperature and salinity data (M: Month, std: Standard deviation, N: Count).

	M8					M11					M14				
M	T40	StdT	S40	StdS	N	T40	StdT	S40	StdS	N	T40	StdT	S40	StdS	N
1	15.4	0.4	38.2	0.4	11	15.3	0.7	37.9	0.6	10	15.5	0.4	37.9	0.6	11
2	15.2	0.3	38	0.4	12	15.1	0.3	37.9	0.3	10	15.3	0.5	37.9	0.3	11
3	14.9	0.6	37.9	0.8	11	14.9	0.6	37.8	0.9	11	15.1	0.5	37.8	0.9	11
4	15	0.6	38	0.9	11	14.9	0.6	38	0.9	10	15.1	0.3	38	0.9	10
5	15.2	0.2	38.4	0.2	13	15.1	0.2	38.3	0.1	11	15.1	0.2	38.3	0.1	11
6	15.2	0.2	38.4	0.1	13	15	0.2	38.3	0.1	12	15.2	0.2	38.3	0.1	12
7	15.1	0.2	38.5	0.1	12	15	0.2	38.3	0.2	12	15.2	0.2	38.3	0.2	12
8	15.1	0.2	38.5	0.1	13	15	0.1	38.4	0.1	13	15.1	0.2	38.4	0.1	12
9	15	0.2	38.5	0.1	12	15	0.2	38.4	0.1	12	15.1	0.2	38.4	0.1	12
10	15.2	0.2	38.4	0.1	11	15.2	0.2	38.3	0.2	11	15.2	0.2	38.3	0.2	10
11	15.3	0.3	38.4	0.1	13	15.4	0.3	38.4	0.1	13	15.3	0.3	38.4	0.1	13
12	15.5	0.5	38.4	0.1	13	15.5	0.5	38.3	0.3	13	15.5	0.4	38.3	0.3	12
	M23					MY1					MY2				
M	T40	StdT	S40	StdS	N	T40	StdT	S40	StdS	N	T40	StdT	S40	StdS	N
1	15.5	0.3	38.4	0.2	10	15.3	0.4	38.1	0.3	10	15.4	0.6	38	0.4	9
2	15.4	0.4	38.2	0.3	10	15.1	0.6	37.9	0.7	10	15	0.5	37.8	0.6	9
3	15.4	0.3	38.3	0.2	11	14.9	0.5	37.9	0.8	11	14.9	0.6	37.8	0.8	10
4	15.1	0.2	38.2	0.3	11	14.8	0.4	37.9	0.8	10	14.9	0.5	37.8	0.8	9
5	15.2	0.2	38.3	0.1	12	15.1	0.1	38.3	0.1	11	15.1	0.1	38.2	0.2	9
6	15.2	0.2	38.4	0.1	12	15	0.2	38.3	0.1	12	15	0.1	38.2	0.1	10
7	15.1	0.2	38.4	0.1	12	15	0.1	38.4	0.1	12	15.1	0.1	38.4	0.1	10
8	15.1	0.2	38.4	0.1	13	15	0.1	38.4	0.1	13	15	0.2	38.3	0.2	10
9	15.1	0.2	38.5	0.1	9	15	0.2	38.4	0.1	12	15	0.2	38.3	0.1	10
10	15.1	0.1	38.4	0.1	11	15.2	0.2	38.3	0.1	11	15.2	0.2	38.3	0.1	10
11	15.3	0.3	38.5	0.1	13	15.3	0.2	38.4	0.1	13	15.5	0.3	38.4	0.1	11
12	15.4	0.3	38.4	0.3	11	15.6	0.5	38.4	0.2	13	15.6	0.6	38.3	0.3	11

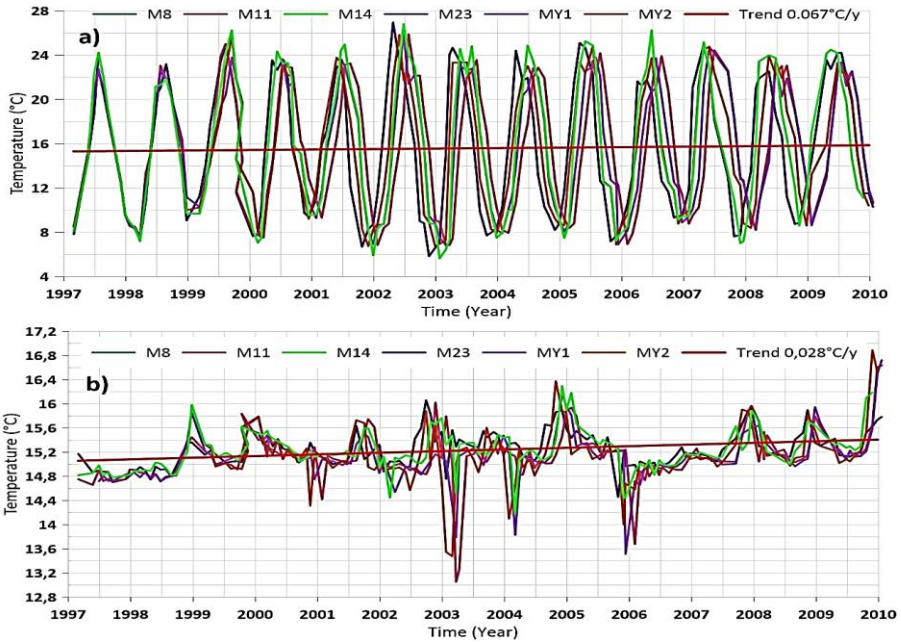

Figure 6. Upper (a) and lower layer sea temperature trends.

Table 5. Trend values of each station

	Temperature (°C)				Salinity (psu)			
	Upper layer		Lower layer		Upper layer		Lower layer	
	Trend	Mean	Trend	Mean	Trend	Mean	Trend	Mean
M8	0.06	15.38	0.03	15.18	0.1	22.01	0.015	38.31
M11	0.08	15.56	0.03	15.14	0.1	23.97	0.008	38.21
M14	0.06	15.94	0.03	15.23	0.13	22.78	0.012	38.34
M23	0.04	15.59	0.03	15.24	0.11	22.84	0.006	38.37
MY1	0.06	15.57	0.03	15.13	0.1	24.14	0.004	37.89
MY2	0.1	15.68	0.02	15.15	0.09	24.01	0.025	38.17
Mean	0.067	15.62	0.028	15.18	0.105	23.29	0.012	38.27

winds occasionally block the lower layer during high sea levels in the Black Sea, while southerly winds block the upper layer during low sea levels, creating what is known as Orkoz (Altıok et al., 2014, Jarosz et al. 2011, Alpar et al., 1998, 1999; Latif et al., 1991; Özsoy et al., 1986). It is possible to observe these anomalies in temperature and salinity values as a consequence of deterioration in the two-layer structure of SoM, as a result of the influence of strong wind conditions. Some of these dates coincide with upper or lower layer blockages, indicating that they were caused by mixing between the two layers during the period of strong winds.

To investigate the dynamic interaction between meteorologic and oceanographic parameters, the comparison between the upper layer sea temperature trend and the air temperature trend is presented in Figure 7. Upon examining the upper layer temperature data of 1997-2010 period, a direct relationship with air temperature is observed. The sea temperature consistently records a 2-3°C elevation relative to the locations of minimum air temperature. At the peaks of air temperature and sea temperature, they had the same values or a difference of 1-2°C. Notably, July 2002, marked by peak seawater temperature, emerged as one of the warmest months. Similarly, February 2003, coinciding with the trough in seawater temperature, exhibited the lowest average temperatures. When the trend values are analyzed, similarities are observed. The annual temperature increase of 0.085°C in the air affected the oceanographic data and caused an annual temperature increase of 0.067°C in the upper layer. The fact that the highest and lowest temperatures for the stations were experienced in the upper layer and were similar to the air temperatures proves that oceanographic conditions are related to atmospheric conditions. Changes similar to atmospheric changes have been observed in the BS surface temperature during the last century (Oguz et al., 2006). These changes in upper layer temperature have also affected the cold interlayer temperature in the BS. Especially BS cold interlayer temperature has increased in parallel with the increase in upper layer temperature since 1993 (Oguz, 2017).

In order to compare the effect of climate change to the upper layer sea temperature in the surrounding seas, an analysis of relevant research was conducted. The collected trends in upper layer sea temperatures are presented in Table 6.

The salinity trends of the upper and lower layers in the study area are depicted in Figure 8. The annual increase in salinity for the upper layer is 0.105 psu. Upper layer salinity values are high in March, November, December 1998, January and December 2001, December 2003, November 2006, December 2007, August, November, December 2008. Interestingly, the M11, MY1, and MY2 stations located in the east of the IS demonstrate consistently higher salinity averages compared to other stations. Lower layer salinity trend is increase of 0,012 psu per year. Lower layer salinity values are low in December 2001, January and March 2002, January, March and April 2003, March 2004, February and March 2006. The station with the highest salinity in lower layer is M23. MS effects are observed more in this station compared to other stations. The properties of lower layer water may also vary spatially and temporally in proportion to the hydrodynamic conditions prevalent throughout the IS.

Table 6. Surrounding seas upper layer temperature trends

Region	Trend (°C)	Date	Method	Reference
SoM	0.07	1997-2010	In-situ observations	This study
IS North Exit	0.07	1996-2010	In-situ observations	Altiok and Kayisoglu (2015)
	0.15			
BS	0.09	1981-2000	Satellite	Ginzburg et al. (2004)
BS	0.052	1982-2020	measurements	Ginzburg et al. (2021)
	0.05	1982-2012		Shaltout and Omstedt (2014)
	0.06	1982-2002		Belkin (2009)
	0.07	1993-2017		E.U. Copernicus Marine Service Information (2018)
AS	0.04	1982-2012	Satellite	Shaltout and Omstedt (2014)
	0.05	1980-2000	measurements	Theocharis (2008)
	0.05	1985-2008		Skliris et al. (2011)
AS	0.01	1955-2015	MEDSEA_REANALYSIS _PHY_006_009 data	Serykh, and Kostianoy, A.G., 2021
MS	No trend	1970-1980	In-situ observations	Lelieveld et al. (2002)
	0.03	1980-2000		
	0.03	1974-2005	Satellite	Vargas-Yanez et al. (2008)
	0.03	1982-2012	measurements	Shaltout ve Omstedt (2014)
	No trend	1985-1996		D'Ortenzio et al. (2000)
	0.04	1985-2008		Skliris et al. (2012)
	0.04	1985-2006		Nykjaer (2009)

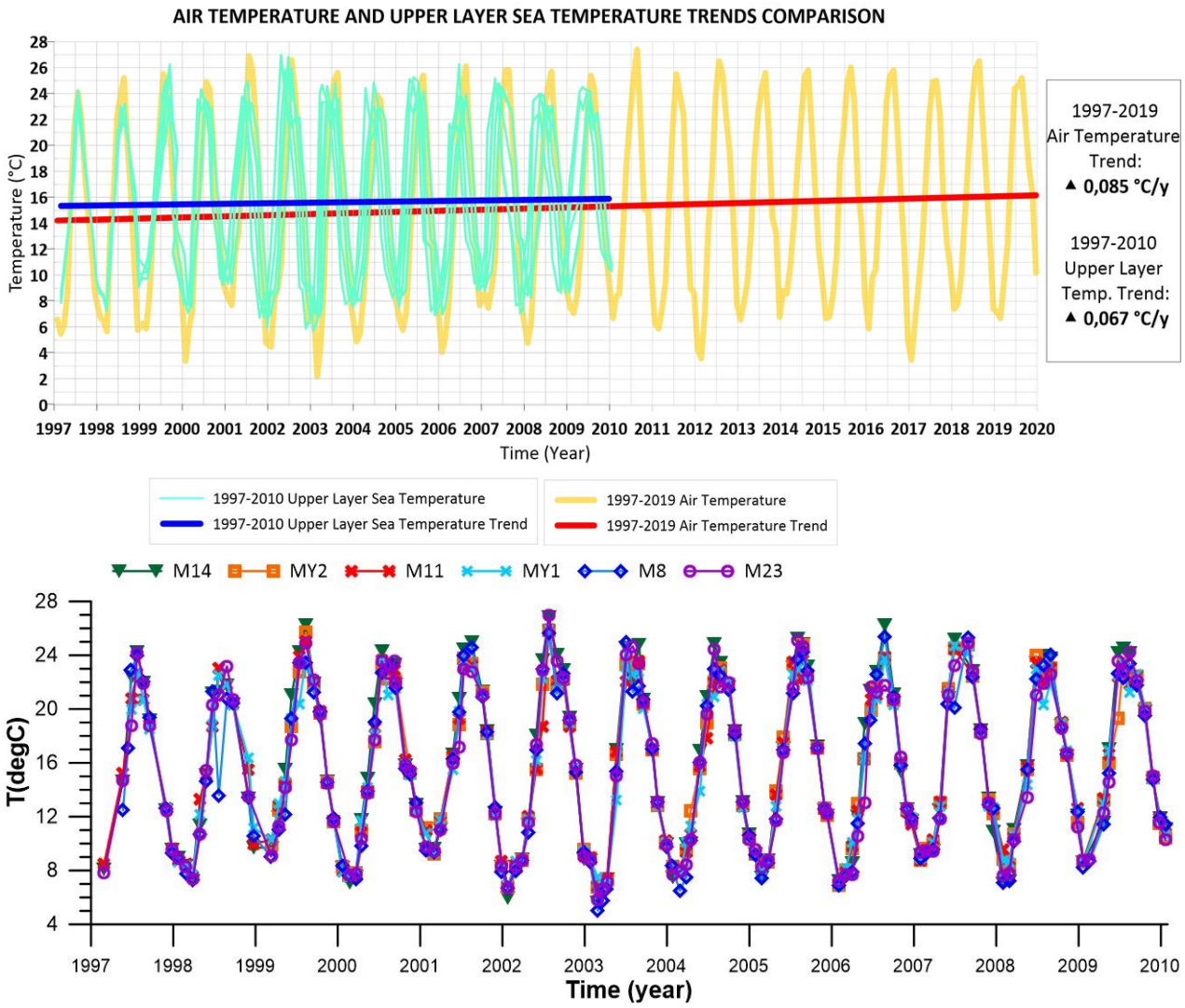

Figure 7. Air temperature and upper layer sea temperature trends comparison

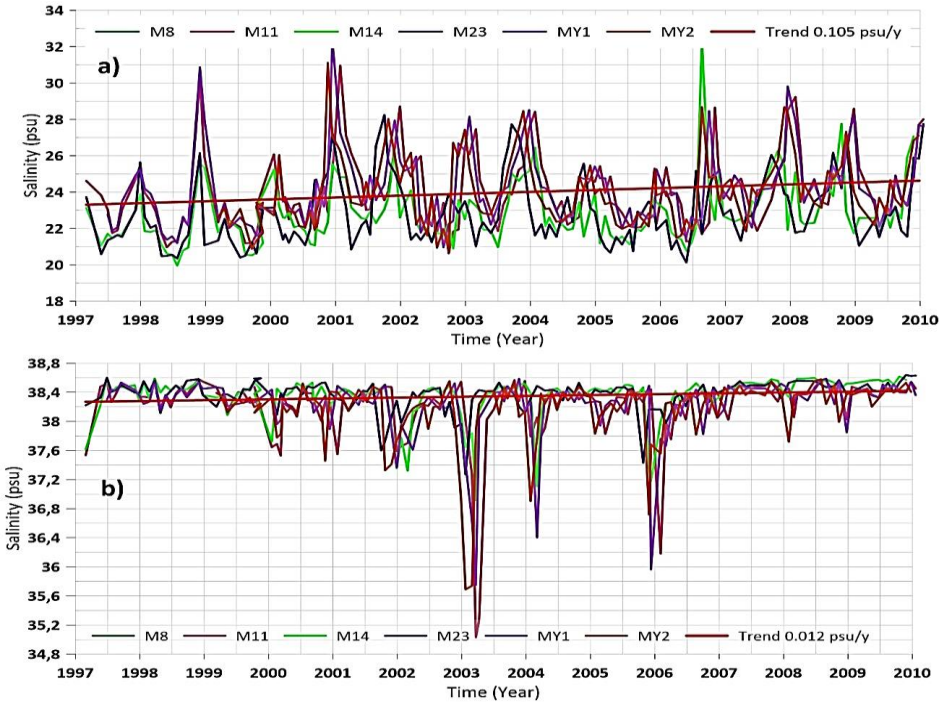

Figure 8. Upper (a) and lower (b) layer salinity trends.

Trend Analysis Results with Recent Data Comparison and Discussion

Comparative analysis was conducted for the MY2 station, located in the east of the Prince Islands. The comparison encompasses 1997-2009 April and October averages and 2019 values of the same months. The findings are visually presented in Figure 9, through the depiction of temperature and salinity profiles. When analyzing the April temperature data, it becomes evident that the data for 2019 surpass the standard deviation values of the 1997-2009 average data in both the upper and lower layers. Additionally, these 2019 values exhibit a narrow range of proximity between the 25th and 40th meter depths. Upon comparing the October temperature data from the identical station, it was noted that a temperature increase was observed in both layers over time, Notably, the measurements within the range of 15 to 25 meters exhibited values closely aligned with those from the preceding period. When the 1997-2009 April and October salinity data of the same station are compared, it is seen that the new values are within the standard deviation of the average of the old period data, and there is an increase only in the first 5 meters in October.

The same study as above was applied to the Cinarcik Basin. Analyzing the upper and lower layer comparisons depicted in Figure 10, it becomes evident that the temperature values in April 2019 exceeded the 1997-2009 average, particularly within the first 10 meters. Beyond the 10-meter mark, the values align with the standard deviation. Upon examining the October data, the 2019 values fall within the standard deviation of the 1997-2009 average data for the first 15 meters. Between the 15th and 25th meters, the values remain within the standard deviation range, while a temperature increase of over 0.5 °C is observed after the 25th meter. Examining the salinity data, both layers exhibit an increase in both April and October, and the new value in the intermediate layer is within the standard deviation of 1997-2009. Throughout all periods at both stations, higher temperature and salinity values were observed in the lower layer during 2019 compared to the maximum values between 1997-2009. In summary, over a span of approximately 10 years, both upper and lower layers at both stations experienced elevated temperatures in April, surpassing the 13-year average and standard deviation. The comparison for October reveals a similar high temperature increase in the lower layer, while the upper layer's temperature remained high but within the standard deviation range. Salinity values were consistently higher in both layers and during both months.

Conclusion

In this study, an analysis was conducted on the temperature and salinity data from east of the SoM stations between 1997 and 2010. Time series were generated, trends and averages for temperature and salinity were calculated. These were then compared with atmospheric trends and oceanographic conditions of neighboring seas. The obtained temperature and salinity trends were examined to understand the impact of climate conditions on oceanographic parameters, with a focus on elucidating the consequences of climate change on these parameters. The necessity of investigating climate change effects on seas prompted the study. While similar investigations had been conducted in surrounding seas, this study marks the first to determine atmospheric and oceanographic parameter trends in the east of the SoM concerning upper and lower layers.

From the obtained values, it is evident that the average temperature trend in the east of the SoM for the upper layer is 0.067°C per year and for the lower layer is 0.028°C per year, both showing a positive increase. The upper layer displayed the highest temperature increase in the east of the IS exit, whereas the lower layer's temperature trend was uniformly distributed throughout the region. The mean temperatures were higher in the west of the IS exit, while the temperature trends were higher in the east of the IS.

Upper layer temperatures reached peaks in August 1999, July 2002, July 2003, and August 2005. Lower layer temperatures peaked in December 2002, December 2004, February 2005, December 2009, and January 2010, while hitting lows in March 2002, March and April 2003, March 2004, February 2006, and March 2010. CIL thicknesses ranged from 5 to 21 meters between May and August. Notably, station M23 representing Cinarcik Basin exhibited the longest persistence of this layer, despite having the lowest thickness.

For salinity trends, the upper layer displayed an average trend of 0.105 psu per year, while the lower layer's trend was 0.012 psu per year. Salinity increased from sea surface to interlayer depth. Upper layer salinity values are high in March, November, December 1998, January and December 2001, December 2003, November 2006, December 2007, August, November and December 2008. The east of the IS exit exhibited higher average salinity in the upper layer compared to other stations. Lower layer salinity values remained consistent across stations. Station M23 held the highest lower layer salinity due to its MS exposure.

To explore atmospheric parameters, data from the Florya Meteorological Station between 1997 and 2019 were utilized. Air temperature was generally lower in January and February, while it peaked in July and August. The coldest month was February 2003, aligning with the lowest surface water temperature. The hottest month was August 2010 with an average of 27.4°C. The rate of exceeding the 25°C temperature threshold increased from 8% in the late 1990s and 2000s to 13% in the 2010s. Furthermore, atmospheric pressure trends indicated higher averages in winter, particularly December-January, and lower averages during summer.

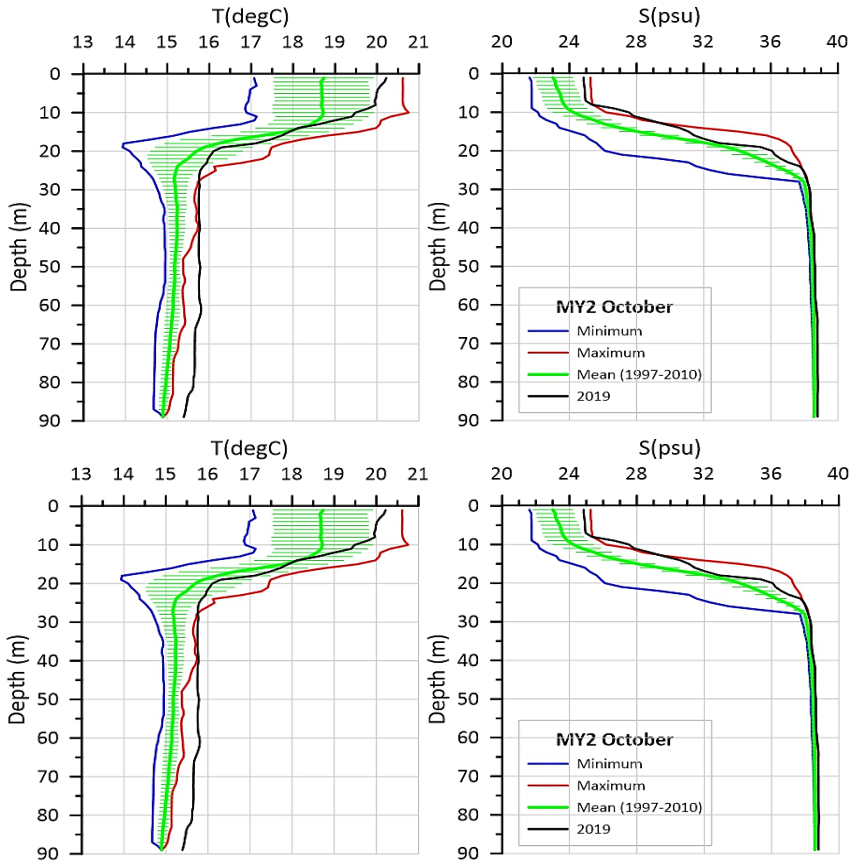

Figure 9. MY2 station temperature and salinity profiles (Green plots represent 1997-2009 mean, light green ones represent standard deviation, blue ones represent minimum, red ones represent maximum values, black plots represent 2019 value.).

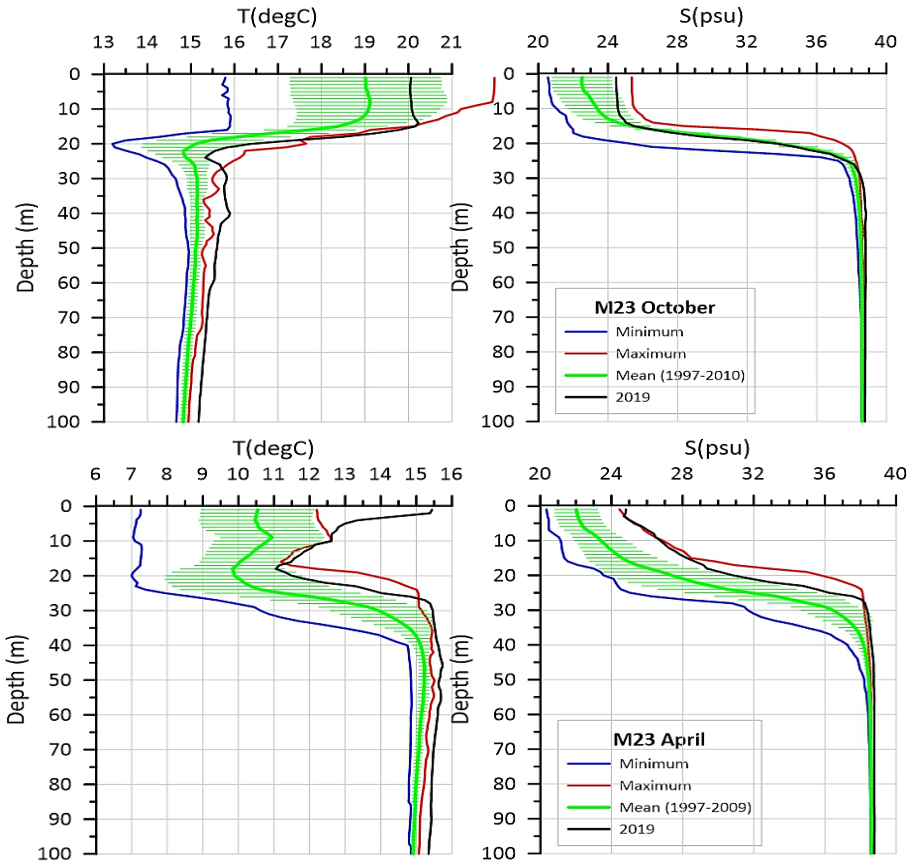

Figure 10. Cinarcik Basin temperature and salinity profiles (Green plots (M23) represent 1997-2009 mean, light green ones (M23) represent standard deviation, blue ones (M23) represent minimum, red ones (M23) represent maximum values, black plots (45C) represent 2019 value.)

Throughout the period spanning 1997 to 2019, the mean pressure threshold of 1020 mbar, responsible for inducing anticyclonic air currents, was surpassed on 8 occasions. Notably, 4 of these instances transpired prior to 2010, with the remaining 4 occurring within the decade of the 2010s. Trend analysis revealed an increase of 0.085°C per year in average air temperature and a decrease of 0.034 mbar per year in average air pressure. The temperature trend between 2010-2019 (0.11°C/year) is approximately twice the trend between 1997-2010 (0.06).

The study observed a direct correlation between air temperature and upper layer temperature. Notably, sea temperature was 2-3°C above the lowest air temperature points and comparable or slightly higher at the highest points. Changes in the upper layer temperature and the CIL were linked to the characteristics of water from the BS. The increase in the BS CIL is in parallel with the increase in SST since 1993 (Oguz, 2017) shows the effects of BS oceanography on the upper layer temperature change in the east of the SoM.

When comparing the calculated trend values to historical trends in the surrounding seas, significant similarities were observed. Similar values were also evident at the northern exit of the IS, whereas contrasting values emerged at the southern exit due to the diversity in the CIL and the mixing of the layers.

Comparing data collected from 1997 to 2010 with 2019 data for the upper and lower layers, in MY2 station and Cinarcik Basin supported the identified temperature and salinity trends.

In conclusion, undeniable global warming necessitate increased oceanographic research to detail their effects on the seas. Expeditions and data collection should intensify, with heightened frequency of trend analyses, and an exploration of whether parameter increases are accelerating. Proactive measures should be taken, acknowledging this as a universal issue.

Ethical Statement

This article does not contain any studies with human or animal subjects. Ethical approval is not applicable for this article.

Funding Information

No funding was received for conducting this study.

Author Contribution

First Author: Conceptualization, Formal Analysis, Investigation, Methodology, Visualization and Writing-review and editing; Second Author: Data Curation, Formal Analysis, Investigation, Methodology, Visualization and Writing

Conflict of Interest

The author(s) declare that they have no known competing financial or non-financial, professional, or personal conflicts that could have appeared to influence the work reported in this paper.

Acknowledgements

Authors acknowledge all scientific personnel and R/V Alemdar staff who take place in data collecting process for their meticulous efforts.

References

Aktan, Y., Dede, A., & Ciftci, P.S. (2008). Mucilage event associated with diatom and dinoflagellates in Sea of Marmara, Türkiye. In *Harmful Algae News* (pp 20). The Intergovernmental Oceanographic Commission of UNESCO, No. 36.

Altiok, H., & Kayisoglu, M. (2015). Seasonal and interannual variability of water exchange in the Strait of Istanbul. *Mediterranean Marine Science*, 16(3), 636-647. https://doi.org/10.12681/mms.1225.

Belkin, M. (2009). Rapid warming of large marine ecosystems. *Progress in Oceanography*, 81(1–4), 207–213. https://doi.org/10.1016/j.pocean.2009.04.011

Besiktepe, S.T., Sur, H.I., Ozsoy, E., Latif, M.A., Oguz, T., & Unluata, U. (1994). The circulation and hydrography of Marmara Sea. *Progress in Oceanography*, 34(4), 285-333. https://doi.org/10.1016/0079-6611(94)90018-3

Danovaro, R., Fonda Umani, S., & Pusceddu, A. (2009). Climate change and the potential spreading of marine mucilage and microbial pathogens in the Mediterranean Sea. *PLoS ONE,* 4(9), e7006. https://doi:10.1371/journal.pone.0007006

D'Ortenzio, F., Marullo, S., & Santoleri, R. (2000). Validation of AVHRR Pathfinder SSTs over the Mediterranean Sea. *Geophysical Research Letters*, 27(2), 241–244. https://doi.org/10.1029/1999GL002357

Edwards, E. (2016). Impacts and effects of ocean warming on plankton. Chapter: 3.2. In: Explaining ocean warming: Causes, scale, effects and consequences. Full report, (eds., Laffoley, D., Baxter, J.M.) Gland, Switzerland: IUCN. pp. 75-86.

E.U. Copernicus Marine Service Information. (2018). *Black sea anomaly time series sea surface temperature.* https://marine.copernicus.eu/access-data/ocean-monitoring-indicators/black-sea-anomaly-time-series-sea-surface-temperature

Ginzburg, A., Kostianoy, A., & Sheremet, N. (2004). Seasonal and interannual variability of the Black Sea surface temperature as revealed from satellite data (1982–2000). *Journal of Marine Systems*, 52(1–4), 33–50. https://doi.org/10.1016/j.jmarsys.2004.05.002

Ginzburg, A.I., Kostianoy, A.G., Serykh, I.V. et al. (2021). Climate Change in the Hydrometeorological Parameters of the Black and Azov Seas (1980–2020). *Oceanology* 61, 745–756. https://doi.org/10.1134/S0001437021060060

Gunduz, M., Ozsoy, E., & Hordoir, R. (2020). A model of Black Sea circulation with strait exchange (2008–2018), *Geosci. Model Dev.*, 13, 121–138. https://doi.org/10.5194/gmd-13-121-2020

IPCC. (2019). Technical Summary. In: H.O. Portner, D.C. Roberts, V. Masson-Delmotte, P. Zhai, M. Tignor, E. Poloczanska, K. Mintenbeck, A. Alegría, M. Nicolai, A. Okem, J. Petzold, B. Rama, & N.M. Weyer (Eds.), *IPCC Special Report on the Ocean and Cryosphere in a Changing Climate* (pp. 39–69). Cambridge University Press, Cambridge, UK and New York, USA. https://doi.org//10.1017/9781009157964.002

Lelieveld, J., Berresheim, H., Borrmann, S., Crutzen, P., Dentener, J., Fischer, H., Feichter, J., Flatau, P. J., Heland, J., Holzinger, R., Korrmann, R., Lawrence, M. G., Levin, Z., Markowicz, K. M., Mihalopoulos, N., Minikin, A., Ramanathan, V., De Reus, M., Roelofs, G. J., … Ziereis, H. (2002). Global air pollution crossroads over the Mediterranean. *Science*, 298, 794–799. https://doi.org/10.1126/science.1075457

Lindsey, R., & Dahlman, L. (2020). *Climate Change: Ocean Heat Content.* https://www.climate.gov/news-features/understanding-climate/climate-change-ocean-heat-content

Miladinova, S., Stips, A., Garcia-Gorriz, E., & Macías, D. (2018). Formation and changes of the Black Sea cold intermediate layer. *Progress In Oceanography*, 167, 11-23. https://doi.org/10.1016/j.pocean.2018.07.002

Nykjaer, L. (2009). Mediterranean Sea surface warming 1985–2006. *Climate Research*, 39, 11–17. https://doi.org/10.3354/cr00794

Oguz T., Dippner J.W., & Kaymaz Z. (2006). Climatic regulation of the Black Sea hydro-meteorological and ecological properties at interannual-to-decadal time scales. *Journal of Marine Systems*, 60, 235-254. https://doi.org/10.1016/j.jmarsys.2005.11.011

Oguz T. (2017). Physical Oceanography. In M. Sezgin, L. Bat, D. Urkmez, E. Arici, B. Ozturk (Ed.), *Black Sea Marine Environment: The Turkish Shelf* (pp. 1-13). Tudav Yayinlari.

Özsoy, E., & Ünlüata, Ü. (1997). Oceanography of the Black Sea: A review of some recent results. Earth-Science Reviews, 42(4), 231-272. https://doi.org/10.1016/S0012-8252(97)81859-4

Philippart, C.J., Anadon, R., Danovaro, R., Dippner, J.W., Drinkwater, K.F., Hawkins, S. J., Oguz, T., O'Sullivan, G., & Reid, P.C. (2011). Impacts of climate change on European marine ecosystems: observations, expectations and indicators. *J. Exp. Mar. Biol. Ecol.*, 400(1–2), 52–69. https://doi.org/10.1016/j.jembe.2011.02.023

Pepler, A. (2023). Projections of synoptic anticyclones for the twenty-first century. *Clim Dyn.* https://dx doi.org/10.1007/s00382-023-06728-4

Schroeder, K., Tanhua, T., Chiggiato, J., Velaoras, D., Josey, S. A., García Lafuente, J., & Vargas-Yáñez, M. (2023). The forcings of the Mediterranean Sea and the physical properties of its water masses. In K. Schroeder & J. Chiggiato (Eds.), Oceanography of the Mediterranean Sea (pp. 93-123). Elsevier. DOI: 10.1016/B978-0-12-823692-5.00005-4.

Shaltout, M., & Omstedt, A. (2014). Recent sea surface temperature trends and future scenarios for the Mediterranean Sea. *Oceanologia*, 56(3), https://doi.org/411–443.10.5697/oc.56-3.411

Serykh, I.V., Kostianoy, A.G. (2021). Climate changes in temperature and salinity of the Aegean Sea. in: the handbook of environmental chemistry. Springer, Berlin, Heidelberg, https://doi.org/10.1007/698_2021_817

Skliris, N., Sofianos, S., Gkanasos, A., Axaopoulos, P., Mantziafou, A., & Vervatis, V. (2011). Long-term sea surface temperature variability in the Aegean Sea. *Adv. Oceanography and Limnology,* 2(2), 125–139. https://doi.org/10.4081/aiol.2011.5321

Skliris, N., Sofianos, S., Gkanasos, A., Mantziafou, A., Vervatis, V., Axaopoulos, P., & Lascaratos, A. (2012). Decadal scale variability of sea surface temperature in the Mediterranean Sea in relation to atmospheric variability. *Ocean Dynamics,* 62, 13–30. https://doi.org/10.1007/s10236-011-0493-5

Theocharis, A. (2008). Do we expect significant changes in the thermohaline circulation in the Mediterranean in relation to the observed surface layers warming? F. Briand (Ed.), *Climate Warming and Related Changes in Mediterranean Marine Biota* (pp. 25-30). Monaco: CIESM.

Tukenmez, E., & Altiok, H. (2022). Long-term variations of air temperature, sea surface temperature, surface atmospheric pressure, surface salinity and wind speed in the Aegean Sea. *Mediterranean Marine Science*, 23(3), 668–684. https://doi.org/10.12681/mms.25770

Unluata, U., Oguz, T., Latif, M.A., & Ozsoy, E. (1990). On the physical oceanography of the Turkish straits. In: L.J. Pratt (Ed.), *The Physical Oceanography of Sea Straits* (pp. 25-60). NATO/ASI series, Dordrecht: Kluwer. https://doi.org/10.1007/978-94-009-0677-8_2

von Schuckmann, K., Le Traon P.Y., Smith, N., Pascual, A., Djavidnia, S., Gattuso, J.P., Grégoire, M., & Nolan G. (2020). Copernicus Marine Service Ocean State Report, Issue 4. *Journal of Operational Oceanography,* 13, 1-172. https://doi.org/ 10.1080/1755876X.2020.1785097

Vargas-Yanez, M., García, M.J., Salat, J., García-Martínez, M.C., Pascual, J., & Moya, F. (2008). Warming trends and decadal variability in the Western Mediterranean shelf. Global and Planetary Change, 63, 177–184. https://doi.org/10.1016/j.gloplacha.2007.09.001